The Generation Mechanism and Some Properties of the X Phase

AUTHOR(S):

MORII, Wataru

CITATION:

MORII, Wataru. The Generation Mechanism and Some Properties of the X Phase. Bulletin of the Disaster Prevention Research Institute 1996, 45(4): 85-98

ISSUE DATE:

1996-03

URL:

http://hdl.handle.net/2433/125013

Bull. Disas. Prev. Res. Inst., Kyoto Univ., Vol. 45, Part 4, No. 392, March, 1996

The Generation Mechanism and Some Properties of the X Phase

By Wataru Morii

(Manuscript received on Nov. 1, 1995, revised on Mar. 6, 1996)

Abstract

The generation mechanism of X_3 was investigated. It was concluded that X_3 is a packet of spheroidal overtones. It was already proved in the previous study that X_1 and X_2 are composed of successive arrivals of converted body waves while X_4 is a packet of spheroidal overtones. From the point of view that X_3 and X_4 can be treated as higher modes, the velocity dispersions of X_3 and X_4 were examined. The results show that group velocities of X_3 and X_4 separate into segments corresponding to the extrema of velocity dispersion curves of some higher Rayleigh modes. It can be said that X_3 and X_4 are composed of Airy phases of some higher Rayleigh modes. As to X_1 and X_2, the relation between the predominant periods and magnitudes was examined. The results exhibited an correlation between them. The predominant periods of X_1 and X_2 are related directly to the duration of the source process. It was also revealed that the predominant periods grow longer under the influence of focusing of seismic rays.

1. Introduction

X phases were first recognized by Jobert et al (1977). Jobert (1978) showed that X_4 (the order 4 repetition of the X phase) could be treated as packet of mantle overtones. In other studies concerned with the X phase [(Emil et al., 1987), (Roult et al., 1984), (Tanimoto, 1987), (Tanimoto, 1988)], each of all the repetitions including X_1 was treated as a packet of spheroidal overtones a priori. However, in the previous paper Morii (1993) pointed out that X phases display a transient process of differentiation of seismic waves leading to the formation of modes. It was also exhibited that X_1 is formed mainly by the focusing of SP waves and X_2 is composed of the successive arrivals of multiple-reflected and -converted body waves.

In the previous paper (Morii, 1993), the generation mechanism of the X_3 was not examined because in the analyzed seismograms the X_3 overlapped with the R_2 and could not be separated successfully. However, since the original nature of the phase X is a transient process as mentioned above, in order to clarify the generation mechanism of the phase X, it must be examined whether the X_3 can be treated as a packet of spheroidal overtones or as body waves. Moreover, it is important to know the properties of the phase X when one attempts to utilize it as data to estimate geophysical parameters.

In this study clarification of the generation mechanism of the X_3 was undertaken, and some properties of the phase X were examined.

2. Data

The seismograms analyzed in this study were recorded by the long period seismic wave observation system operating at the Osakayama Crustal Deformation Observatory (situated in the central part of Kinki district, hereinafter abbreviated "OSK") and at the Amagase Observatory (situated to the south of OSK about 13 Km away, hereinafter abbreviated "AMA"). The observation system is composed of a seismograph (a set of seismometers and a signal conditioner unit), an A/D converter unit, a clock, a visual recorder, a hard disk unit and a computer. The computer controls the entire system for data acquisition, using a triggering algorithm. Details of the observation system operating at OSK were mentioned in the previous paper (Morii, 1993). The observation system operating at AMA is similar to the one operating at OSK except for the frequency response characteristics of the seismograph. The frequency response characteristics of the seismographs are shown in Figure 1. Seismometers operating at the both observatories are velocity meters of the moving coil type. As was mentioned in the previous paper, phase- and amplitude-distortion caused by the response characteristics of the seismographs are able to be corrected with a "deconvolution filter" (Kulhanek, 1976). Events from which seismograms analyzed were recorded are listed in Table 1 and great circle paths from epicenter to the observatory are shown in Figure 2. The seismograms from events 1 and 8 in Table 1 were recorded at OSK and those from the other events were recorded at AMA. In this study the velocity records corrected for the response characteristics of the seismographs were analyzed.

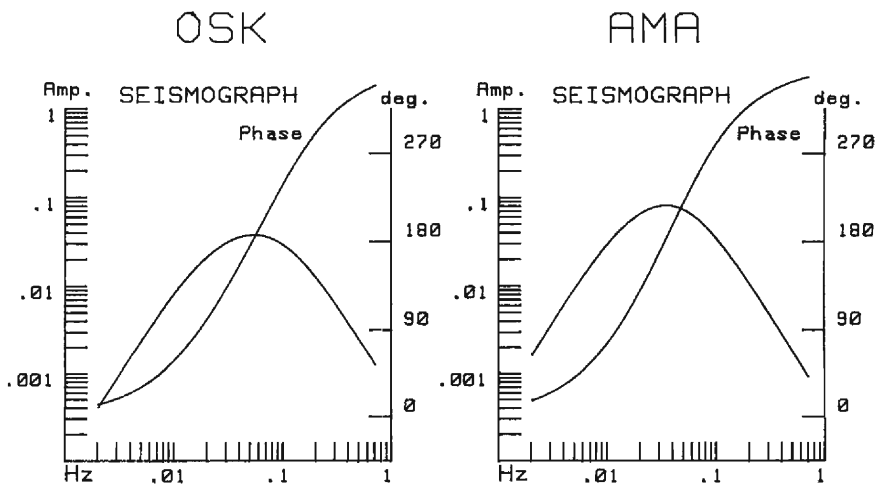

Fig. 1 Frequency response characteristics of the seismographs in operation at OSK and at AMA.

TABLE 1

No.	Origin time (JST)	Location	Depth (in Km)	M	Distance (in Km)	Rzimuth
1	Dec 01 1983 02:46:00.6	06.852S 72.110E	10	7.7	8110.2	248.7
2	Rug 18 1991 07:17:14.6	41.821N 125.397W	14	7.1	8166.1	50.4
3	Apr 26 1992 03:06:04.2	40.368N 124.316W	15	7.1	8329.8	51.2
4	Jun 28 1992 20:57:34.1	34.201N 116.436W	1	7.6	9296.9	52.6
5	Jun 18 1994 12:25:19.5	42.864S 171.465E	33	7.1	9342.1	154.5
6	Sep 11 1993 04:12:54.6	14.71N 92.645W	34	7.3	12519.9	51.7
7	Jul 13 1994 11:35:55.8	16.625S 167.509E	33	7.4	6610.1	144.2
8	May 23 1989 19:54:46.3	52.341S 160.568E	10	8.2	9980.2	165.1

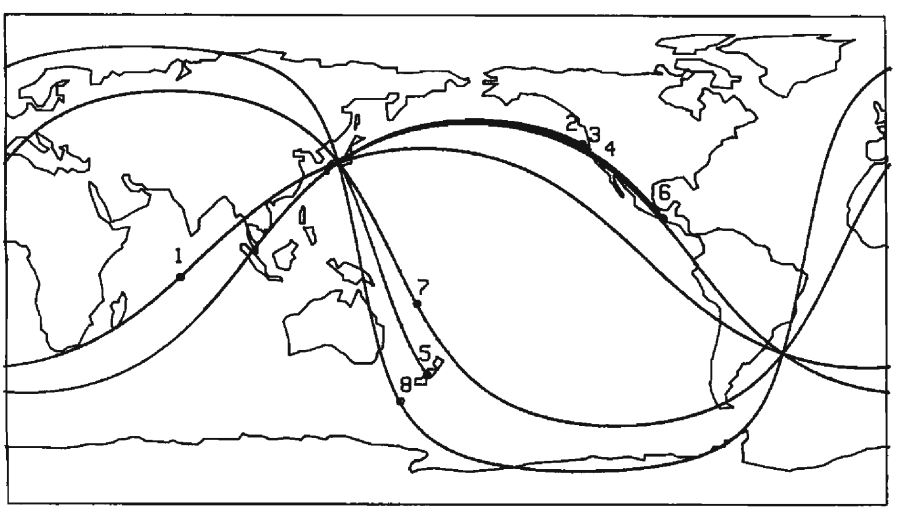

Fig. 2 The great circle paths corresponding to the records analyzed.

3. The generation mechanism of X_3

In Figure 3 the seismogram analyzed to examine the properties of X_3 is shown. This seismogram was recorded from event 7 in Table 1. The epicentral distance from event 7 to AMA is 6610.1 Km. For this epicentral distance, the difference of the arrival time between X_3 and R_2 was large, so that they were recorded separately. In Figure 3, band-pass filtered records in the period range from 40 to 150 seconds are shown, so that each phase on the seismogram is easily identifiable visually. As is shown in the figure, X_3 is sufficiently isolated from R_2. Though the arrival time of X_3 was close to that of G_2, vectors of the oscillation between them were orthogonal. Then, the X_3 could be separated from the G_2 using a coordinate transformation. After the transformation the correlation coefficients between the radial and transverse components were estimated in the period range from 30 to 250 sec. In the time interval containing G_2, the correlation coefficients were less than 0.1. This result may prove that X_3 was separated successfully from G_2.

3. 1. Spectra

The amplitude spectra of X_3 are shown in Figure 4. In order to compare with the amplitude spectra of the other order repetitions of the phase X, those of X_1, X_2 and X_4 are exhibited together in this figure. The amplitude spectra of X_1, X_2 and X_4 were estimated with the seismogram recorded at OSK from the May 23, 1989 Macquarie Ridge earthquake listed in Table 1 as number 8. The curves shown in Figure 4 were normalized to the maximum amplitude individually and do not display the amplitude ratios between X_1, X_2, X_3 and X_4.

As is shown in the figure, with regard to the amplitude spectra X_3 is similar to X_4 rather than X_1 or X_2. Especially in the period range shorter than 80 seconds, X_3 and X_4 are nearly identical in amplitude spectra. The amplitude spectra of X_3 have largest peak in the period range from 100 to 115 seconds and a secondarily large peak in the period range from 70 to 80 seconds.

As is shown in Figure 1, the great circle path from event 7 to the observatory is different from the one for event 8. For event 8, almost the entire path runs through the oceanic area. On the other hand, for event 7, about a quarter of the great circle path runs through the continental area.

It follows that the velocity structure along the path for event 7 may differ from the one for event 8, so that the difference of the velocity structure may cause variation of the wave form . However, lateral heterogeneity of the velocity structure which affects wave forms of the higher modes in the period range longer than 100 seconds is less than several percent. In the period range longer than 100 seconds, the variation of the wave form of the higher modes caused by the velocity anomalies is so small as it can be treated by the linear inversion methods [(Tanimoto, 1987), (Tanimoto, 1988)].

Thus, the variations of the amplitude spectra shown in Figure 4 may be caused mainly by the difference of the generation mechanism among X_1, X_2, X_3 and X_4.

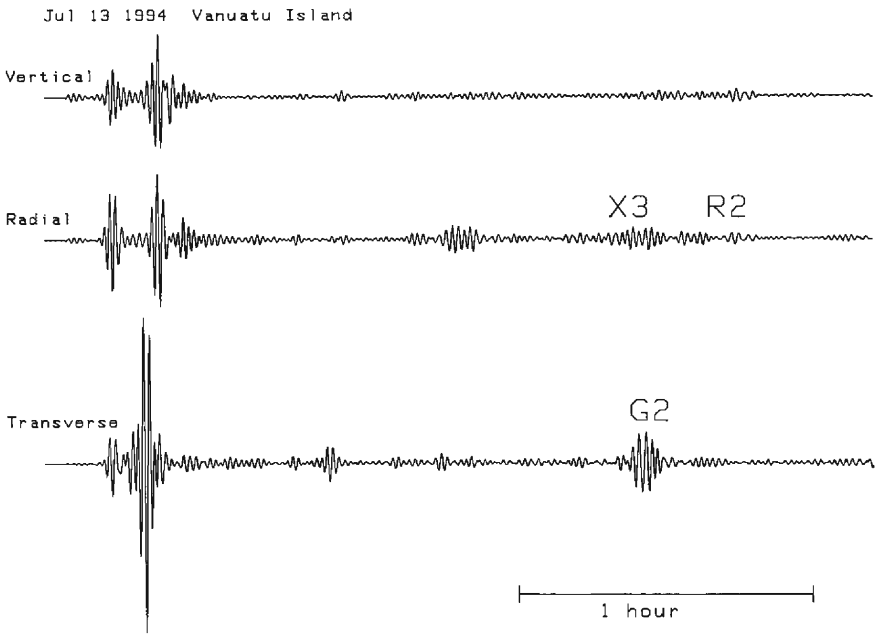

Fig. 3 Vertical, longitudinal and transversal components of the seismogram used for examination of X_3. Seismograms are produced by performing a band–pass filtering operation in the period range from 40 to 150 seconds and a coordinate transformation.

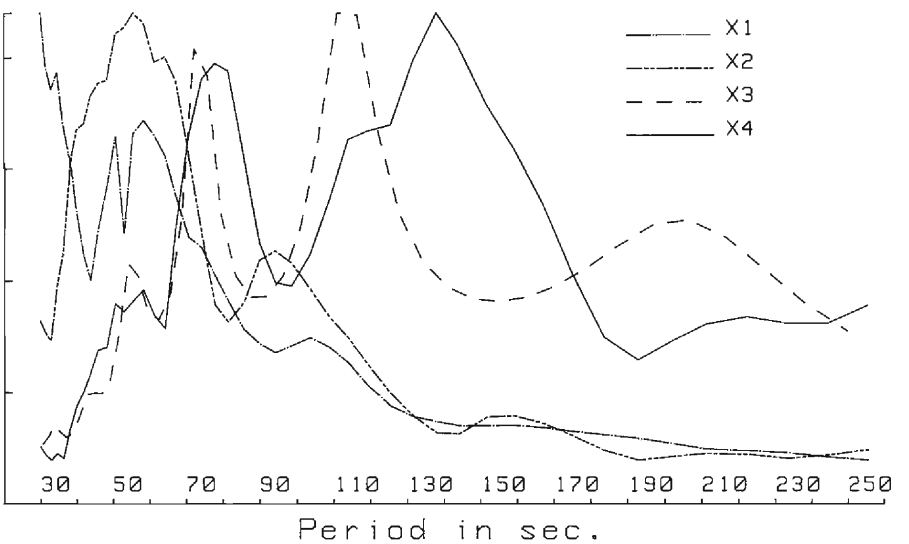

Fig. 4 Amplitude spectra of X_1, X_2, X_3 and X_4. Curves are normalized individually and do not display amplitude ratio among them.

3. 2. Oscillation

At first, it was attempted to treat X_3 by breaking it down into several converted body waves. On the record of X_3, it was attempted to identify converted body waves with reference to the travel times and particle orbits. However, no evident phase of the converted waves, mSnP, was identifiable. Judging from this result and the features of the amplitude spectra, it may be adequate to treat X_3 as a packet of overtones. Following the method used by Jobert (1978), it was then attempted to explain the features of oscillation of X_3 as the superposition of spheroidal overtones. Unit impulse function was used as the source time function. Seismograms for each higher Rayleigh mode from the first to the 11th order were synthesized individually with some Earth model. Summing them up, the X_3 record was synthesized. Figure 5 shows the result. The upper record is the radial component of the X_3 produced from the observed one by performing a low-pass filtering operation at 90 seconds and a coordinate transformation. The observed record was corrected with the deconvolution filter and it can be considered that there is no effect of the frequency response characteristics of the seismograph (Morii, 1993). Lower record was synthesized from the higher mode branches, ${}_3R$, ${}_4R$, ${}_5R$ with PEM-A model (Dziewonski et al., 1975). As is shown in the figure, close agreement between observed and synthesized seismogram was obtained.

As is shown in Figure 4, the amplitude spectra of X_3 have a secondarily large peak

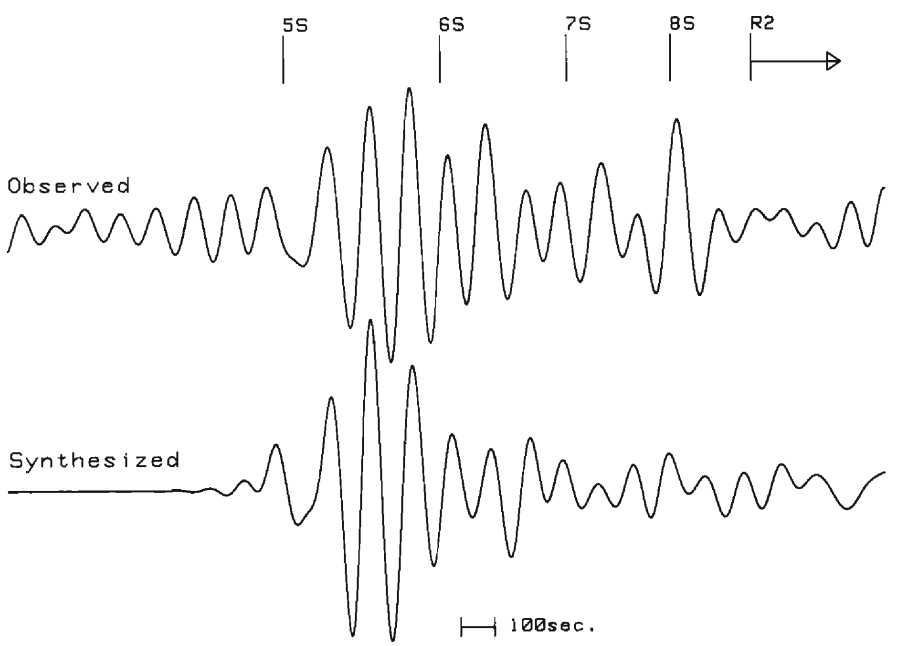

Fig. 5 Comparison between observed and synthesized seismogram of X_3. Travel times of the phases are indicated by the arrival times of the multiple reflected S-waves.

in the period range shorter than 90 seconds. However, in this period range the synthesized seismogram similar to the observed one could not be obtained. In this period range overtone branchs, ${}_5R\sim{}_{11}R$, have extrema with similar group velocities and each extreme value independently varies with changes of the Earth model. Thus, in the period range shorter than 90 seconds, the form of the synthesized seismogram may be affected significantly by even a slight change of the Earth model.

As for X_3, features of oscillation could not be explained by the successive arrivals of converted body waves. No evident phase of mSnP could be identified. It is impossible to treat X_3 by breaking it down into several converted body waves. On the other hand, principal phases could be explained by the superposition of some higher Rayleigh modes. Therefore, it may be adequate to treat X_3 as a packet of spheroidal overtones.

4. Properties of the phase X

As is evident from the results revealed in the previous study, X_1 and X_2 are able to be treated as the body wave. On the other hand, it may be adequate to treat X_3 and X_4 as a packet of spheroidal overtones.

Therefore, the properties of X_1 and X_2 may be different from those of X_3 and X_4 in quality. Then, it may be reasonable to examine the properties of X_3 and X_4 as the different problem from the examination for X_1 and X_2.

4. 1. Group velocities of X_3 and X_4

It was attempted to obtain group velocities of X_3 and X_4 with "multiple filter technique" (Dziewonski et al., 1969). Group velocities of X_3 were estimated with the seismogram recorded from the event 7 in Table 1 while the seismogram from event 8 was used for the estimation of group velocities of X_4. The results obtained are shown in Figure 6. In the figure, theoretical curves of group velocities of some higher Rayleigh modes estimated with PEM-A model, ${}_2R$, ${}_3R$, ${}_4R$, ${}_5R$, ${}_6R$, were exhibited together. As is shown in Figure 6, group velocities obtained from observed seismograms separate into some segments. However, each segment corresponds to extrema of some theoretical curves except for the segment of velocities of the X_3 in the period range longer than 165 seconds.

As for X_4, in the period range shorter than 80 seconds, observed group velocities correspond with the theoretical curve of ${}_6R$; in the period range from 95 to 160 seconds, with the curve of ${}_5R$; and in the period range longer than 170 seconds, with the curve of ${}_3R$. As for X_3, in the period range shorter than 80 seconds observed group velocities correspond with the theoretical curve of ${}_6R$ much more than in the case of X_4. In the period range from 95 to 165 seconds, observed group velocities of X_3 correspond with the curve of ${}_5R$. In the period range from 135 to 165 seconds, observed group velocities of X_3 have intermediate values between ${}_5R$ and ${}_4R$.

Since in this period range, the group velocities of ${}_5R$ are close to those of ${}_4R$, it is probable that the narrow band-pass filter used for evaluation of group velocities could not separate ${}_5R$ from ${}_4R$. In the period range longer than 165 seconds, observed group

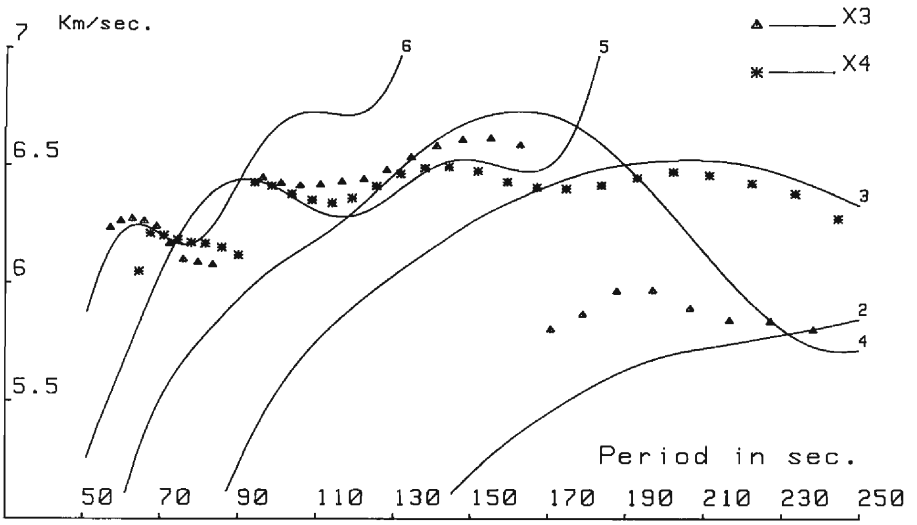

Fig. 6 Observed group velocities of X_3 and X_4. Theoretical curves show the velocity dispersion of the higher Rayleigh modes.

velocities of X_3 are not in agreement with any theoretical curves. As is shown in Figure 4, the amplitude spectra of X_3 has a third large peak in the period range longer than 170 seconds.

However, the extreme value of this peak is fairly small compared with those of the largest and the secondary large maximum. Therefore, it is probable that the narrow band-pass filter used for evaluation of group velocities could not separate ${}_2R$ from ${}_4R$ (Dziewonski et al., 1969). Another probability is that values obtained in this period range were fixed on calculation because of the low S/N ratios (Dzieownski et al., 1969).

In the previous section, it was attempted to synthesize a seismogram coincident with the observed record of the X_3. A successful result could not be obtained in the period range shorter than 90 seconds. However, in this period range good agreement between the theoretical curve and observed group velocities was obtained. In the period range longer than 100 seconds, only three or four higher mode branches contribute to X_3. However, in the period range shorter than 90 seconds, X_3 may contain higher mode branches, ${}_5R\sim{}_{11}R$. It follows that, in the shorter period range, slight variation of group velocities of higher mode branches may cause a considerable change of the wave form of X_3. On the other hand, observed group velocities are estimated by identifying the arrival time of the wave packet with largest energy in each period. Thus, it may be possible that the group velocities of the higher Rayleigh modes with the large energy are extractable from a complicated seismogram. Thus, the fact that the observed group velocities of X_3 correspond to the theoretical curve of ${}_6R$ in the period range shorter than 90 seconds may prove that X_3 can be treated as a packet of overtones also in the period range shorter than 90 seconds.

4. 2. Predominant periods of X_1 and X_2

As was revealed in the previous paper, X_1 and X_2 are composed of successive arrivals of converted body waves. Therefore, the predominant periods of X_1 and X_2 may be affected by source process. The duration of the source process may especially have influence upon the predominant periods of X_1 and X_2. The relation between the predominant periods and the duration of source process of X_1 and X_2 was then examined. The data used were radial components of the seismograms recorded from the events 1 to 6 in Table 1.

They are shown in Figure 7 after a band-pass filtering operation in the period range from 30 to 150 seconds. On the seismograms X_1 or X_2 are clearly identifiable. Since these seismograms were recorded with a triggering algorithm, the duration of each seismogram was determined by its own signal level.

It is a difficult problem in itself to evaluate precisely the duration of a source process. Therefore, the empirical relation between the magnitude and duration of a source process was utilized as the first approximation.

As is shown in Figure 7, six records of X_1 and two records of X_2 were obtained. Amplitude spectra were evaluated with these records and are shown in Figure 8. The periods corresponding to the maximum of the amplitude spectra were taken as predominant. In Figure 9 the relation between magnitudes and predominant periods is exhibited. The theoretical curve shown in Figure 9 indicates the duration of a source process estimated by the empirical relation. The predominant periods of the X_1 and the X_2 from the Macquarie Ridge earthquake ($M=8.2$) were obtained from the amplitude spectra shown in Figure 4. The results exhibit an adequate correlation between magnitude (probably the duration of the source process) and the predominant periods. Predominant periods increase from 30 to 60 seconds in accordance with the increment of magnitudes from 7.1 to 8.2. On the other hand, among three events of similar magnitude ($M=7.1$), the difference between the predominant periods was less than 3 seconds.

As is well known, the factors that mainly control the predominant period of the long period body wave are the duration of the source process and the directivity. The effects of directivity were estimated. The rupture velocity and the length of faulting were estimated by an empirical relation with the magnitude. The strike and the dip angle of the fault were presumed with the source parameters that were reported by U. S. G. S. The direction of the propagation of the rupture is unknown. Using these parameters, the maximum effect of the directivity as much as possible was then estimated.

The maximum effect was obtained in the case of event 4. In this case, the influence of the effect of the directivity on the predominant period is about 9 seconds. However, as for event 4, the predominant period of X_1 is similar to one of X_2. In practice, the effect of the directivity in the case of event 4 may be very small. For the other events, the probable changes of the predominant period caused by directivity are less than 4 seconds.

As mentioned above, X_1 is generated mainly by the focusing of SP waves.

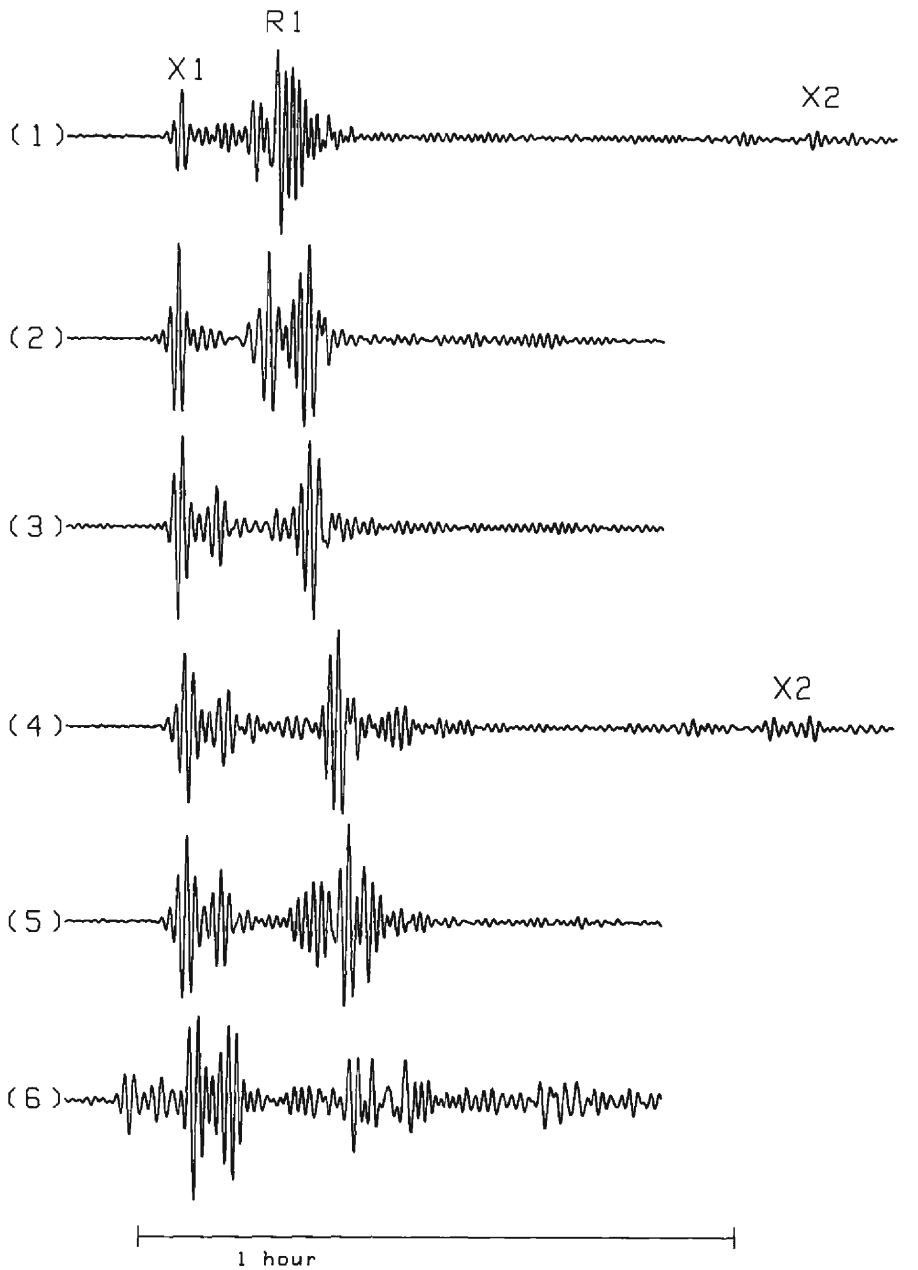

Fig. 7 Radial components of the seismogram used for examination of the X_1 and X_2. Seismograms are produced by performing a band-pass filtering operation in the period range from 30 to 150 seconds and a coordinate transformation. Numbers correspond to the event number listed in Table 1.

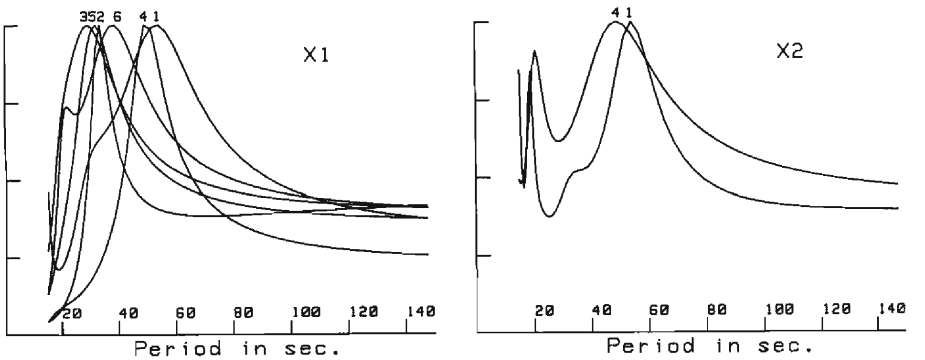

Fig. 8 Amplitude spectra of the X_1 and X_2. Numbers correspond to the event numbers in Table 1.

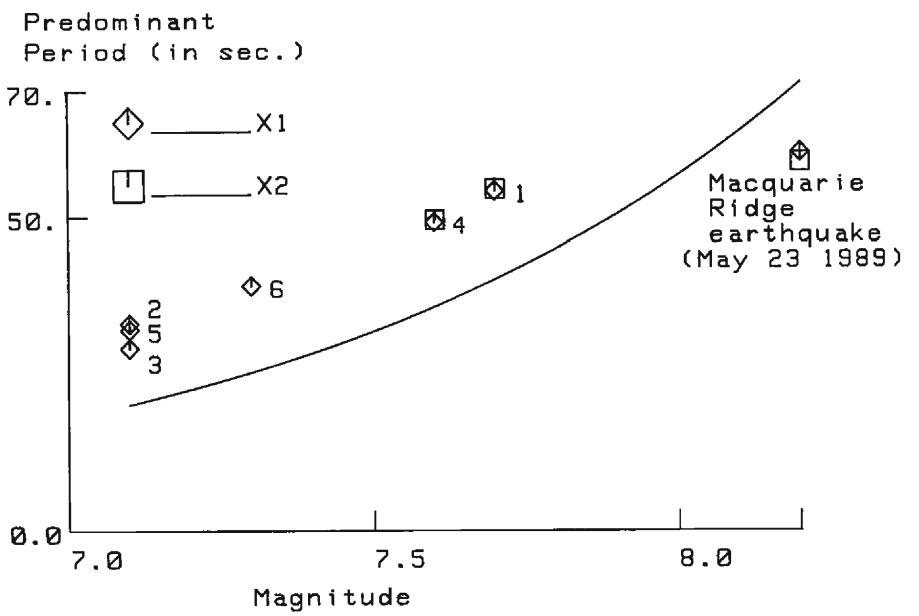

Fig. 9 The relation between magnitude and predominant period. Theoretical curve indicates the duration of the source process estimated with an empirical relation.

Therefore, X_1 is composed of successive arrivals of SP waves which were radiated from a source with different emergent angles and propagated along different paths with different travel times. In the case of $\triangle = 90°$, the difference of the travel times is about 12 seconds in muximum. In Figure 10, some examples of the extension of the pulse width caused by focusing are shown. One cycle of a sinusoidal wave was assumed as the pulse radiated from a source. The pulses phases of which were shifted one another were superimposed. The phase shifts were then evaluated taking into account the difference of the travel time among seismic rays of different

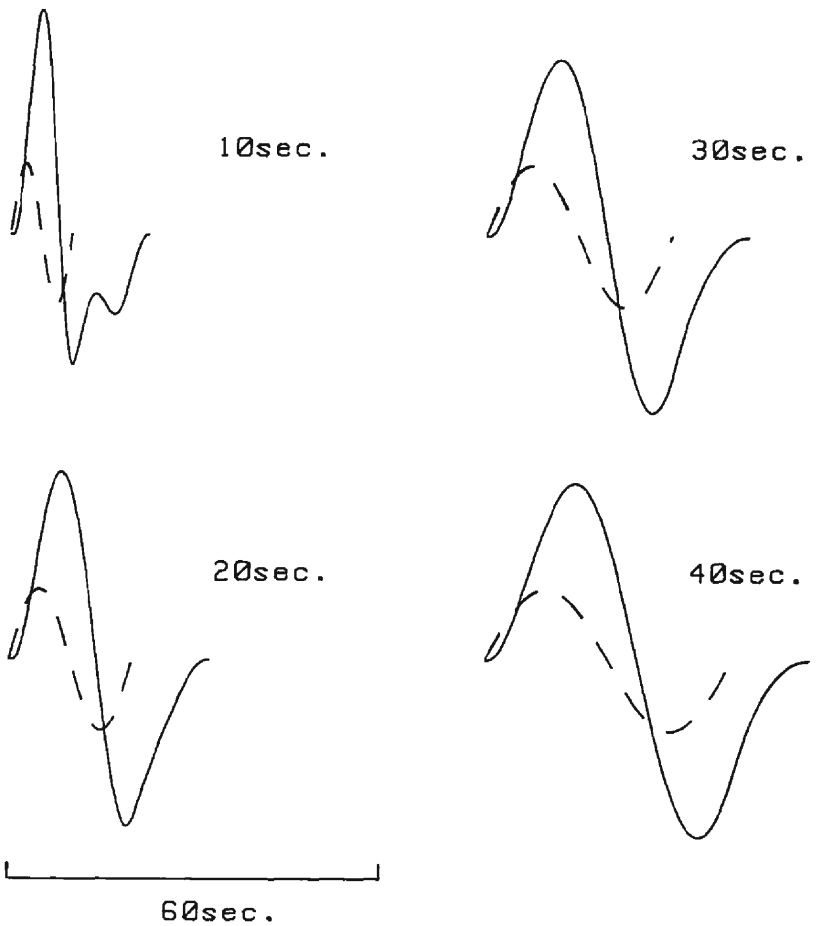

Fig. 10 Examples of the extension of the pulse width caused by the focusing of the SP-wave. The pulses shown by the solid line were composed of the successive arrivals of the pulses shown by the dotted line.

emergent angles. The travel times of each seismic ray were calculated with the PEM-A model (Dziewonski et al., 1975). Four different cases for the duration of the pulse, 10, 20, 30, 40 seconds, were examined. As is shown in Figure 10, when the duration of the pulse was longer than 20 seconds, the duration of the signal formed by superposition grew longer successfully with the wave form of the signal being quasisinusoidal.

Assuming that the predominant period of X_1 and X_2 would grow longer in the same manner as in the above case of the superposition of sinusoidal waves, the difference between the predominant period and the duration of the source process can be explained by the effect of the focusing of seismic rays with different travel times.

5. Discussion

As the main feature of the phase X, it was demonstrated that X_3 is a packet of spheroidal overtones. As is shown in Figure 6, the observed group velocities of X_3 and X_4 coincide with the extrema of some higher mode branches, ${}_3R$, ${}_5R$, ${}_6R$. It can be said that X_3 and X_4 are composed of the successive arrivals of the Airy phases of some higher Rayleigh modes. Therefore, the properties of the X_3 and the X_4 are considered to be controlled mainly by the resonant properties of the Earth. In the case of this study, the feature of the amplitude spectra of X_3 was different from that of X_4 in the longer period range. This may be caused by the difference of the magnitude of the events from which the data for X_3 and X_4 were obtained. X_4 was recorded from an event of Ms=8.2 and X_3 was recorded from one of Ms=7.4. Therefore, the energy of long period components radiated from the source may be fairly different between X_3 and X_4. As to the group velocities of X_3 in the period range longer than 165 seconds, the disagreement between the observation and theory may also be explained by the same reason. In the longer period range, the S/N ratios of the record of X_3 may not be sufficient to estimate observed group velocities. It is likely that the results obtained for X_3 in the period range longer than 160 seconds have no meaning.

It was also demonstrated that the predominant periods of X_1 and X_2 are related directly to the durations of the source process. It is probable that the predominant periods grow longer under the influence of focusing of seismic rays with different travel times. The results revealed are in agreement with the conclusion of the previous paper that X_1 and X_2 are composed of the successive arrivals of the converted body waves and they are affected considerably by the properties of the source process and by the relative position of the seismic source and the observation station. In the case of Macquarie Ridge earthquake, the predominant periods of X_1 and X_2 are shorter than the duration of the source process estimated with the empirical relation. This may be caused by the fact that the rupture propagated bilaterally from the nucleation point (Ekstrom et al., 1990).

6. Conclusion

The properties of the phase X were investigated. Spectra, travel times and the features of the oscillation were examined in detail. The results are as follows:

(1) X_3 is a packet of spheroidal overtones.
(2) Group velocities of X_3 and X_4 separate into some segments. Each segment corresponds with extrema of the theoretical curves of ${}_3R$, ${}_5R$, ${}_6R$.
(3) The predominant periods of X_1 and X_2 are related directly to the duration of the source process. The predominant periods grow longer under the influence of the focusing of seismic rays.

Acknowledgments

The author wishes to express his sincere thanks to Mr. K. Shigetomi for his support and continuous encouragement throughout this work, and critical reading of the manuscript. The author also thanks Drs. T. Furuzawa and K. Matsunami for their continuous encouragement and critical reading of the manuscript.

Reference

Dziewonski, A. M., S. Bloch and M. Landisman: A Technique for the Analysis of Transient Seismic Signals, Bull. Seism. Soc. Am., Vol. 59, No. 1, 1969, pp. 427–444.

Dziewonski, A. M., A. L. Hales and E. R. Lapwood: Parametrically simple earth models consistent with geophysical data, Phys. Earth. Planet. Int., 10, 1975, pp. 12–48.

Ekstrom, G. and B. Romanowicz: The 23 May 1989 Macquarie Ridge Earthquake: A very broad band analysis, Geophys. Res. Let., Vol. 17, No. 7, 1990, pp. 993–996.

Emile, A. Okal and Bong–Gon Jo: Stacking inversions of the dispersion of higher order mantle Rayleigh waves and normal modes, Phys. Earth Planet. Int., 47, 1987, pp. 188–204.

Jobert, N., R. Gaulon, A. Dieulin and G. Roult: Sur des ondes a tres longue periode, caracteristiques du manteau superieur, C. R. Acad. Sc. Paris, t. 285, ser. B-49, 1977

Jobert, N.: Contribution of some particularities in the dispersion curves to numerical seismograms computed by normal modes, J. Comput. Phys., 29, 1978, pp. 404–411.

Kulhanek, O.: Introduction to Digital filtering in Geophysics (Developments in Solid Earth Geophysics 8), Elsevier Scientific Publishing Company 1976.

Morii, W.: On the generation mechanism of the X phase, Bull. Disas. Prev. Res. Inst., Kyoto Univ., Vol. 43, 1993, pp. 41–59.

Roult, G. and B. Romanowicz: "Very long–period data from the Geoscope Network" Preliminary results on great circle averages of fundamental and higher Rayleigh and Love modes, Bull. Seism. Soc. Am., Vol. 74, No. 6, 1984, pp. 2221–2243.

Tanimot, T.: The three–dimensional shear wave structure in the mantle by overtone waveform inversion–I. Radial seismogram inversion, Geophys. J. R. Astr. Soc., 89, 1987, pp. 713–740.

Tanimot, T.: The 3–D shear wave structure in the mantle by overtone waveform inversion–II. Inversion of X–waves, R–waves and G–waves, Geophys. J., 93, 1988, pp. 321–334.